DOI: 10.1007/s12541-012-0234-9

Autonomous Terrain Adaptation and User-Friendly Tele-Operation of Wheel-Track Hybrid Mobile Robot

Yoon-Gu Kim[1], Jeong-Hwan Kwak[1], Dae-Han Hong[1], In-Huck Kim[1], Dong-Hwan Shin[1], and Jinung An[1,#]

1 DGIST, 50-1, Sang-ri, Hyeonpung-myeon, Dalseong-gun, Daegu, Korea, 711-873
Corresponding Author / E-mail: robot@dgist.ac.kr, TEL: +82-53-785-4610, FAX: +82-53-785-4659

KEYWORDS: Wheel-track hybrid, Terrain-adaptive, Intuitive steering, Mobile robot, Transformable structure

This paper presents a terrain-adaptive wheel-track hybrid robot that uses a pair of combined wheel and track systems. The hybrid mobile platform can change the shape of track to adapt to various terrains so that it is able to move fast on flat terrain and to show good performance in overcoming stairs or obstacles. The proposed platform consists of an ordinary wheel structure for fast navigation on flat floors and a transformable tracked structure for climbing stairs effectively. In detail, three track arms installed on each side of the platform are used for the navigation mode transition between flatland navigation and stair climbing. The mode transition is determined and implemented by the adaptive driving mode control of the mobile robot. This wheel-track hybrid mobile platform is evaluated through experiments that assess its navigation performance in real and test-bed environments. This hybrid mobile robot is embodied to perform given tasks in a hazardous environment for surveillance, reconnaissance, and search and rescue applications.

Manuscript received: April 5, 2012 / Accepted: August 5, 2012

NOMENCLATURE

N_a = reaction force on edge point A of the stair
N_b = reaction force on edge point B of the stair
F_a = force working on edge point A
F_b = force working on edge point B
F_{ax} = the X-component of F_a
F_{ay} = the Y-component of F_a
m = mass of the robot platform
d = length of the robot platform
p = height of a stair
r_w = radius of driving wheel
M_b = ascending moment
θ = attack angle
k = length of track arm
r = radius of track wheel

1. Introduction

Natural and complex disasters have become increasingly destructive in many regions of the world. During the past decade, various types of public safety and rescue robots have been developed to search for and rescue victims and to enter collapsed or hazardous buildings and public facilities during disaster situations.[1-4] These types of robots need to have the mobility to crawl over piles of rubble, up and down stairs and up steep ramps. They must also go through extremely small openings and take advantage of pipes, tubes, and other unconventional routes to reach their destinations.[5] The surfaces that they must traverse may be composed of a variety of materials, including carpeting, concrete blocks, wood, and/or other types of construction materials. The surfaces may also be highly unstable.

To overcome these types of terrain, a number of studies on optimal mechanisms for mobile robot platforms have done over the past several decades. There are three main types of robot mobility mechanisms: wheel, leg, and track structures. The wheel structure is advantageous when a mobile robot is navigating on flatland, but it is difficult for the robot to overcome unstable ground conditions such as stairs and unpaved roads with this structure. Leg-structured robots can navigate with a high degree of adaptability to various environments, but they have disadvantage in terms of energy efficiency and navigation speed. Furthermore, these types of robots are difficult to control stably under complex ground conditions.[6] The track structure shows better performance and stability under complex conditions, but it also has disadvantage in terms of energy efficiency and navigation speed. For example, CALEB-2,[7] RobHaz[8] and PackBot[9] use the track mechanism to cope with various ground conditions. Based on these complementary points of view, we considered a wheel-track hybrid mobile robot platform for quick navigation on flat floors and with good performance when climbing stairs. There are several wheel and track hybrid robot platforms.[10-12] Galileo Mobility Instruments (GMI) and Elbit Systems co-developed the small portable mobile robot platform known as VIPeR (Versatile, Intelligent, Portable Robot).[13] In addition, Lee presented a small robot based on a hybrid wheel-track mechanism. It employs a clutch mechanism to shift between the wheel and the track drive modes.[14] The AZIMUT robotics platform from Sherbrooke University uses leg-track-wheel articulations that provide omni-directional locomotion. It is designed to navigate both flat surfaces and uneven terrain.[15] The Shrimp III[16] is a research platform with extended climbing abilities instilled by its passive mechanical configuration. The passive structure makes it possible for this robot to climb obstacles without actively sensing them. Instead, it simply moves forward and lets its mechanical structure adapt to the terrain profile.

Because special consideration has been given to flexibility for real applications, we designed a transformable mobile platform structure for a wheel-track hybrid type platform that is comprised of an ordinary wheel for quick navigation over flat floors and a transformable track to climb stairs effectively. The proposed mobile platform has an adaptive driving mode control that can select either the wheel mode or the track mode. It is applicable to variable urban environments.

This paper is organized as follows. Section 2 presents the design and implementation of the wheel-track hybrid robot platform. Its adaptive driving mode control is described in Section 3. Experimental results and performance analyses are discussed in Section 4. Finally, the conclusions are given in Section 5.

2. Design and Implementation of the Wheel-track Hybrid Platform

The ultimate aim of this work is to implement a practical mobility mechanism by merging the respective advantages and offsetting the disadvantages of both wheel and track structures. For the purpose, we attempted to devise a mobility mechanism for a mobile robot that satisfies both simplicity of the mechanical structure and adaptability to various terrains. The proposed wheel-track hybrid robot platform aims at simultaneously rapid driving over flat terrains and good climbing of stairs or ramps. To determine the optimal size and shape of the tracks for climbing stairs or ramps, the necessary parameters for ascending stairs are derived and then applied to the design and implementation of the wheel-track hybrid robot platform. The design concept and embodiment process of this wheel-track hybrid mobile robot platform have been updated by being based on our previous researches.[17,18]

2.1 Design concept of the wheel-track hybrid robot platform

The wheel and track should be geometrically configured so as to be able to navigate and be adaptable to any terrain condition, such as flatland, stairs, and unpaved roads. Thus, three configurations were designed to drive the robot platform in different modes, as shown in Fig. 1. The flatland navigation mode, Fig. 1(a), is a wheel-driving track configuration for flatland. In this mode, two tracks of the robot are folded without ground contact and four wheels are driven in contact with the ground. Thus, the robot can move rapidly on a floor without friction between the tracks and the ground. Ascending and descending modes are represented in Figs. 1(b) and (c), respectively. In these modes, two tracks are unfolded while keeping the four wheels from coming into contact with the ground. Therefore, only the two tracks are in contact with the ground, which enables the robot crawl over piles of rubble, up and down stairs, and up steep ramps in a stable manner. In the ascending mode, the tracks can be adaptively transformed according to the height of the obstacles. In the descending mode,

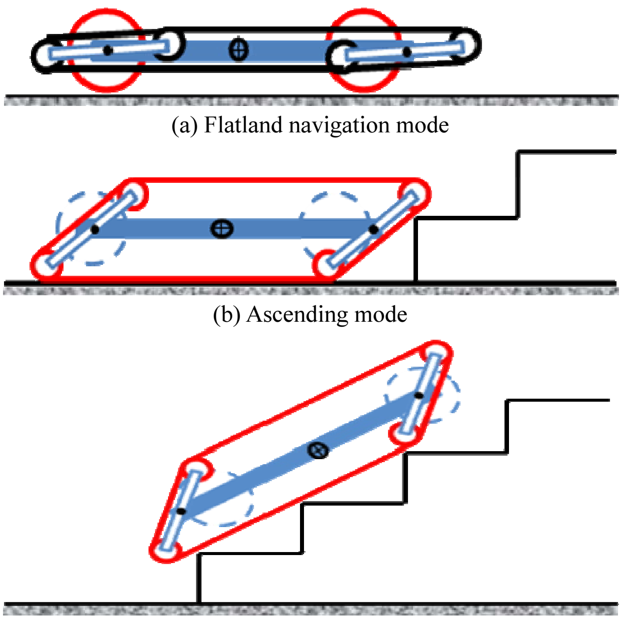

Fig. 1 Conceptual design of the robot platform

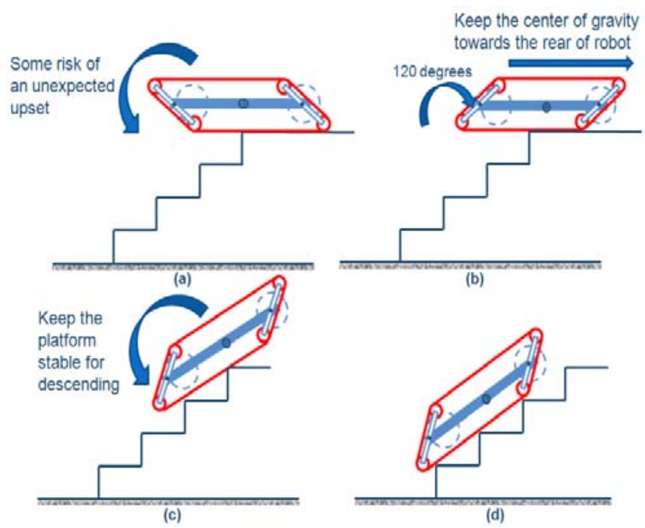

Fig. 2 Procedure of descending stairs

the tracks are transformed backwards at about 120 degrees so that the robot maintains its center of gravity towards the rear. This makes the descending mode stable without the risk of an unexpected upset. The slope of stairs in general buildings is generally less than 35 degrees. The transformable track angle range is 10 to 150 degrees. Thus, this transformable platform can cover the slope range of typical stairs. The procedure of descending stairs is depicted in Fig. 2. Further details pertaining to the implementation are described in the next section.

2.2 Implementation of the wheel-track hybrid robot platform

Figure 3 shows a free body diagram (FBD) of the wheel-track hybrid robot platform in the ascending mode. As soon as the robot attacks the stairs with a set attack angle (θ), the robot climbs the stairs instantaneously. It is thus possible to assume that the acting forces are mainly concentrated on the first attacked point (**A**) and on the rear contact point (**B**). Given that the platform has to overcome and climb the stairs after attacking, the moment (M_b) should be maximized.

The force equilibrium is described in (1).

$$\begin{aligned}\Sigma F_x = 0;\ \mu N_a \cos\theta - N_a \sin\theta + \mu N_b = 0\\ \Sigma F_y = 0;\ \mu N_a \sin\theta + N_a \cos\theta + N_b - mg = 0\end{aligned} \tag{1}$$

From (1), the reaction forces, N_a and N_b, are obtained.

$$\begin{aligned}N_a &= \frac{\mu mg}{(1+\mu^2)\sin\theta}\\ N_b &= \frac{(\sin\theta - \mu\cos\theta)mg}{(1+\mu^2)\sin\theta}\end{aligned} \tag{2}$$

If the force working on point **A** is denoted as F_a, the *X*- and *Y*-components of F_a are represented as follows:

$$\begin{aligned}F_{ax} &= \mu N_a \cos\theta - N_a \sin\theta\\ F_{ay} &= \mu N_a \sin\theta + N_a \cos\theta\end{aligned} \tag{3}$$

Here, k denotes the length of the track arm and r denotes the radius of the track wheel. Finally, the moment (M_b) can be expressed as follows (4):

$$M_b = -pF_{ax} + (d + p\cot\theta)F_{ay} - \frac{1}{2}mg\left(d + k\cos\theta\right). \tag{4}$$

As mentioned above, gaining the maximum moment is preferable to an easier ascension of the stairs. Equation (5) is derived from (2), (3) and (4).

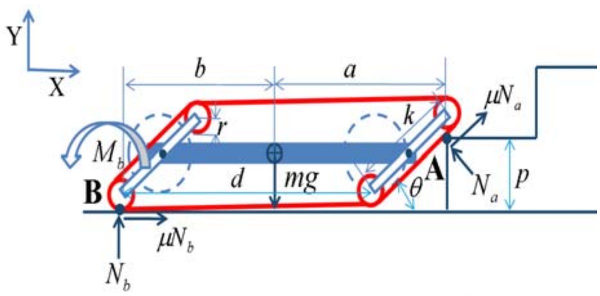

Fig. 3 Parameters of the ascending mode

$$\begin{aligned}M_b = \frac{mg}{1+\mu^2}\Bigg[&\mu\left(1+\cot^2\theta\right)p + \left(\frac{\mu^2-1}{2} + \mu\cot\theta\right)d\\ &-\frac{\mu^2+1}{2}k\cos\theta\Bigg].\end{aligned} \tag{5}$$

As a performance measure, this equation can be used to determine the design parameters. Equation (6) is used to determine the optimal parameters that maximize M_b to the greatest extent possible. The restriction parameters are mass of the robot platform (m) 30 kg, length of the robot platform (d) 0.8 m, height of a stair (p) 0.18 m, and radius of the driving wheel (r_w) 0.12 m. As a result, the optimal parameters are ascending moment (M_b) 133.14 Nm, approaching angle (θ) 36 degrees, length of the track arm (k) 0.27 m, and radius of the track wheel (r) 0.06 m. The conditions for the restriction parameters are shown below:

$$\begin{aligned}&k\sin\theta > p,\\ &k/2 > r,\\ &r_w > r.\end{aligned} \tag{6}$$

The wheel-track hybrid robot platform was developed as shown in Fig. 4. This robot platform is driven by four motors: a pair of motors for the wheel drive and another pair of motors for the track drive. Each motor is accompanied by an individual driver. The main control unit is composed of an embedded controller and several micro-controller unit (MCU) modules; we used a LabVIEW® based development environment for the upper controller applications, which include basic navigation speed and steering control, autonomous driving mode control, and ambient environment acquisition schemes. Each MCU module has its own function, such

(a) Track driving mode (b) Wheel driving mode

Fig. 4 The wheel-track hybrid robot platform

Table 1 Specification of the wheel-track hybrid robot platform

Item	Specification
Dimensions	1,070 × 600 × 343 mm (fully opened track) 1,146 × 600 × 240 mm (fully folded track)
Net weight	50 kg (including 2 batteries: 2 kg)
Payload	20 kg
Transformable track angle	10 to 150 degrees
Max. forward speed	2.16 km/h (track), 7.32 km/h (wheel)
Climbing capability	40°
Steering method	Skid steering
Motor	24 V and 150 W (nominal speed 6930 rpm, reduction ratio 43:1)
Battery	24 V and 6 Ah × 2 EA
Sensors	PSD sensor, Ultrasonic module, gyro sensor, Laser range-finder (URG-04LX, Hokuyo), IP camera (Axis 213 PTZ)

as obstacle detection/avoidance and range/attitude data acquisition for terrain-adaptive navigation. This platform has a camera, a laser range finder, an ultrasonic module, a position-sensitive detector (PSD) sensor, and a gyro sensor. It is possible for the wheel-track hybrid mobile platform to drive at a maximum forward speed of 7.2km/h in the wheel driving mode and at 2.16km/h in the track driving mode. The net weight of this platform is approximately 50kg, and it can handle a payload of about 20kg. Table 1 presents the specifications of the robot platform.

3. Terrain-Adaptive Navigation and User-Friendly Tele-Operation

Terrain-adaptive capability is one of the major advantages of the presented wheel-track hybrid robot platform. The robot has to determine the attack angle to climb over obstacles it encounters in very harsh urban environments. In order to estimate the attack angle of obstacles, three pairs of PSD infrared sensors are installed at each different height on the front of the robot body. Each pair of PSD sensors detects the distances from the obstacle individually as confronted by the mobile platform. As a result, the attack angle can be calculated according to the geometric relationship of the detected distances and the heights of the installed sensors. The wheel-track hybrid robot is highly adaptable and able to move over any terrain by the autonomous attack angle estimation of obstacles. Table 2 and Figure 5 show the estimation of the attack angle (θ) and the height (H) according to the detected distances from obstacles. The different heights of the installed sensors, h_1, h_2, and h_3, are 60, 160, and 260mm from the ground, respectively. d_1, d_2, and d_3 are the detected distances at each height, and ND means no detection. The robot can transform the track as much as the estimated attack angle. Figure 6 shows the deployment design of the PSD sensors, which have valid detection distances ranging from 30cm to 150cm. The distance measuring operation time of the PSD sensor is 38.3ms±9.6ms and the distance measuring resolution is about 0.2cm using a 10-bit ADC within the valid measurement distance range. An MCU (ATmega8) is included for the adaptive driving control scheme.

Table 2 Estimation of the obstacle angle and height

Obstacle distances	θ	H
$d_1 \approx d_2 \approx d_3 \approx$ ND	Wheeled navigation	Flat
$d_1 < d_2$ and $d_3 \approx$ ND	$\arctan\left(\frac{h_2 - h_1}{d_2 - d_1}\right)$	h_2
$d_1 >\approx d_2$ and $d_3 \approx$ ND	$\arctan\left(\frac{h_2}{d_2}\right)$	h_2
d_1 and $d_2 \approx d_3 \approx$ ND	$\arctan\left(\frac{h_1}{d_1}\right)$	h_1
$d_1 < d_2 < d_3$	$\arctan\left(\frac{h_3 - h_1}{d_3 - d_1}\right)$	h_3
$d_1 >\approx d_2$ and $d_2 < d_3$	$\arctan\left(\frac{h_3 - h_2}{d_3 - d_2}\right)$	h_3
$d_1 > d_3$ or $d_2 > d_3$	$\arctan\left(\frac{h_3}{d_3}\right)$	h_3
$d_3 <\approx h_3$	Obstacle avoidance	Over h_3

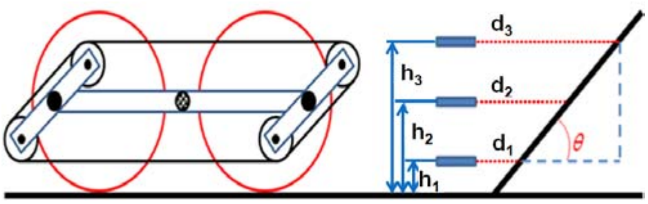

Fig. 5 Sensor location for the estimation of the attack angle

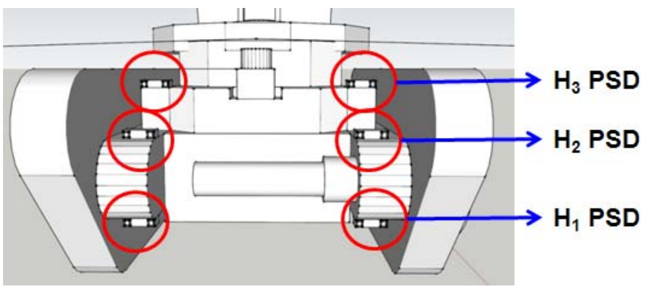

Fig. 6 Deployment design of the PSD sensors

The robot could be semi-autonomous in that it could be remotely operated if an operator helps it to carry out its mission. It is thus necessary to determine how to control the robot easily at a long distance. A user-friendly remote controller was developed for this. It can intuitively show the robot's heading to the operator, as shown in Fig. 7(a). In order to make simple steering decisions, combining the depth information from a laser range-finder, a camera, and an ultrasonic sensor is proposed. Projecting laser range data and the distance data onto a colored texture image can guide an operator to steer the robot in the desirable directions, as depicted in Fig. 7(b).

Each radial contour interval represents a distance of 500mm, and the radial lines are spaced at 15 degrees. Through sensor fusion of the laser finder and the ultrasonic sensor, the depth information overlaid onto the image is marked as the red dotted line. To assist with the steering guidance when the robot suddenly encounters moving obstacles or somewhat narrow paths, haptic feedback is additionally presented to the operator through the joystick. Varying the frequency and the amplitude of the vibrating motor according to the distance to the obstacles, operators can easily maneuver the robot through any harsh environment.

(a) (b)

Fig. 7 User-friendly remote controller and intuitive steering decision

4. Experimental Results

An experimental test of the wheel-track hybrid robot platform was carried out in test and actual environments. Figure 8 shows the installation of the PSD sensors and the test environments were built as shown in Figs. 9 and 10. They consisted of a steel slope, a steel staircase, and a wooden staircase. The first experiment examined the slope and the stair-climbing performance. When the robot ran into obstacles and went over them, attack angle estimation was necessary for the robot to transform the track. The attack angle was easily estimated using the rules shown in Table 2. As soon as the minimum value among the distances measured by the six PSD sensors was within 100cm, the robot started unfolding the track. When the estimated angle arrived at a steady state, the robot stopped transforming the track.

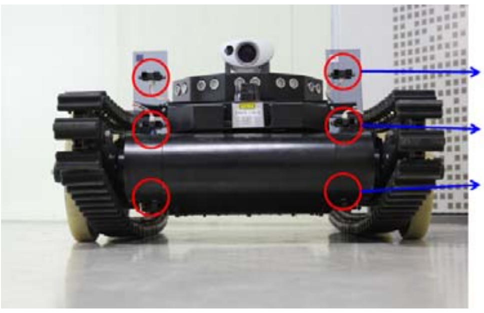

Fig. 8 Installation of the PSD sensors

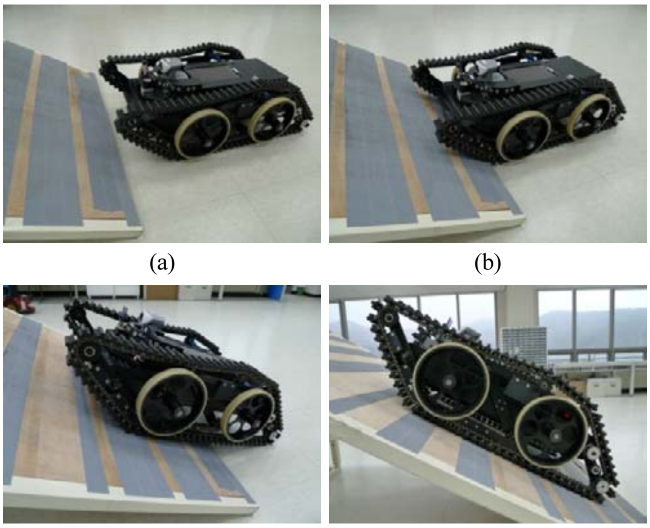

(a) (b)

(c) (d)

Fig. 9 Experiment on a slope with a gradient of 30 degrees

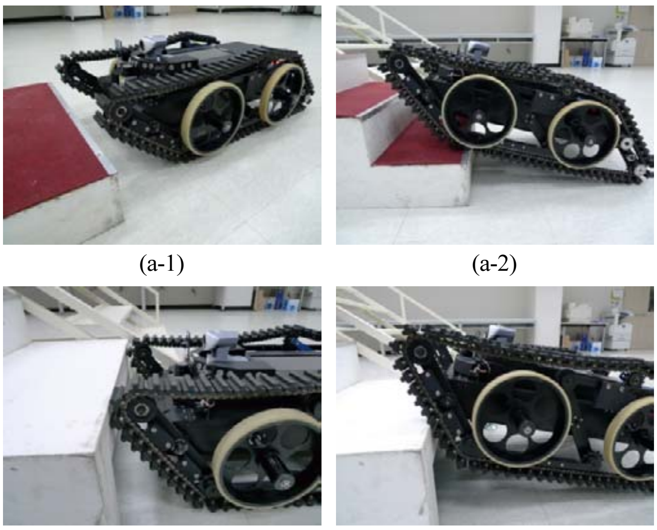

(a-1) (a-2)

(b-1) (b-2)

Fig. 10 Experiment of climbing up a test-bed with stairs 0.16m high (a) and a vertical obstacle 0.27m high (b)

The robot moved over the 30 degrees slope without any slippage, as pictured in Fig. 9. In the next part of the experiment, the robot was tested as it climbed a staircase. Different from when it climbed the slope, estimation of an adequate attack angle was necessary for the robot to transform the track, as it had to mount the first step. The other experimental case was one in which the robot had to overcome test-bed stairs with a height of 0.16m, as shown in Fig. 10. The robot approaches the first step of the stairs and detects obstacle distances through the PSD sensors installed at both sides of

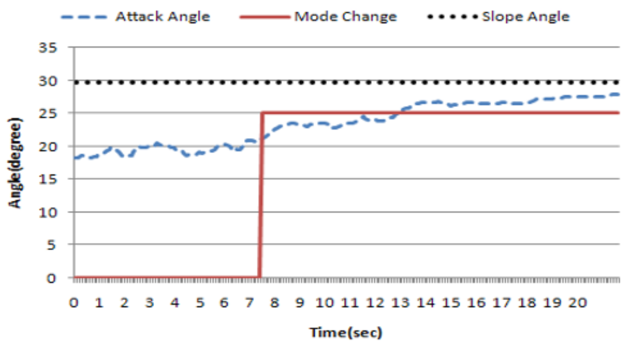

(a) Slope 30°

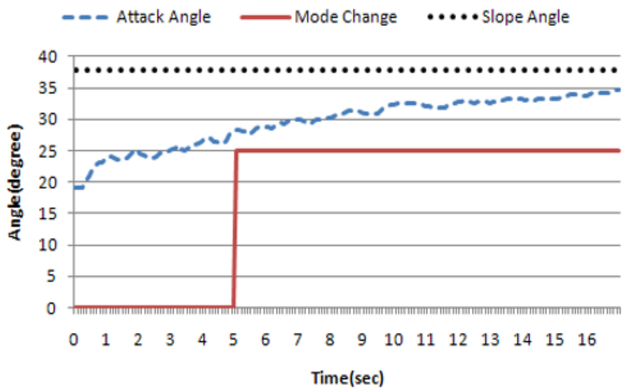

(b) Slope 38°

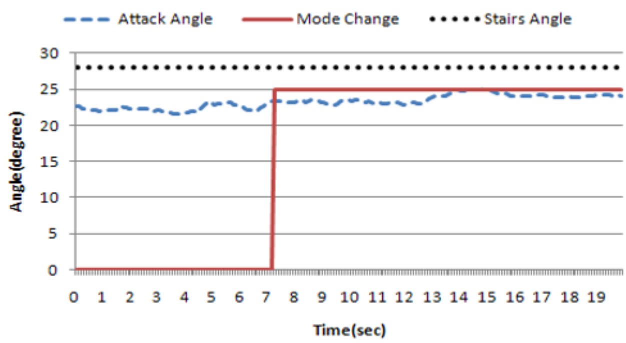

(c) Test-bed stairs 28°

Fig. 11 Autonomous attack angle estimation the platform. After estimating the attack angle to overcome the stairs, the robot transforms the track attitude according to the estimated attack angle and climbs the first step. The remaining stairs are no longer a factor in the track attitude transformation.

Figure 11 shows the results of the autonomous attack angle estimation. Each case of experiment was performed as to a slope 30° (a), a slope 38° (b), and a test-bed stairs 28° (c). When the minimum value among the distances measured by the six PSD sensors is within 100cm, the mode change, which the robot starts unfolding the track, is started at about t = 7 (a), t = 5 (b), and t = 7 (c) in Fig. 11, respectively. As the robot approaches the front of stairs, the estimated angle comes at a steady state so that the robot stops transforming the track and starts climbing up the stairs or slope. The estimated attack angles of each case are plotted in the experimental result graph of Fig. 11. As a result, most of the experimental results verified the error of the estimated attack angles is within 5 degrees. The discrepancy between the real slope gradient and the estimated angle was caused by the difference in the distance measurement error as detected by each sensor. For a more accurate determination of the attack angle, the sensitivity of the sensors needs to be calibrated against the minimum and maximum detection distances to approximate the measured values to the real precise unit distances through the application of Lagrange interpolation or a regression analysis. As a result of the performance tests of the proposed wheel-track hybrid robot platform, the robot was verified to have the ability to climb stairs or vertical obstacles with a maximum gradient angle of 40 degrees and a maximum height of roughly 270mm, as shown in the experiment results presented in Fig. 10(b).

To obtain the empirical results pertaining to the performance of the robot on the wheeled mode, we determined how fast the hybrid robot platform could navigate an arbitrary straight-line path of 10m in our laboratory. We used different RPM speeds with the robot and measured the time for it to arrive at the finish line. The navigation experiments, performed on the actual floor were performed at 500, 1000, and 2000 RPM, respectively. We intended to estimate the proportional maximum speed in the wheel mode through empirical results at the low speeds. The navigation experiments were run three times at the same speed, and we acquired the elapsed time and the average RPM during each trial of 10m of navigation. As a result, the proportional maximum speed can be calculated proportionally, as follows:

$$\begin{aligned} &\text{Proportional Max. Speed(m/h)} \\ &= \text{Speed(m/sec)} \times 60\text{(sec)} \times 60\text{(min)} \times \text{(Nominal RPM)} \\ &\quad /\text{(Measured Avg. RPM)}. \end{aligned} \tag{7}$$

The maximum navigation speeds of each mode are calculated using the measured speed, as shown in Tables 3 and 4. The current driving RPM is acquired from each motor driver at an interval of 100ms during the navigation of 10m straight-line path. As a result of the speed measurement, we estimated that the maximum actual speed is approximately 7.322km/h in the wheel mode and 2.162km/h in the track mode. Furthermore, the turning radius of the robot platform does not exceed 70cm when the track is unfolded.

Table 3 Navigation speed measurement in the wheel mode

Commanded RPM (Wheel mode)	500 RPM			1000 RPM			2000 RPM		
Trial count	Trial 1	Trial 2	Trial 3	Trial 1	Trial 2	Trial 3	Trial 1	Trial 2	Trial 3
Measured Avg. RPM	502.99	499.81	498.75	1004.89	1006.28	1005.11	1988.15	1998.79	2003.47
Speed (m/sec)	0.14706	0.14662	0.14642	0.29412	0.29412	0.29332	0.58824	0.58824	0.59151
Proportional Max. Speed (m/h)	7294.08	7318.59	7324.10	7301.95	7291.86	7280.43	7381.36	7342.08	7365.65

Table 4 Navigation speed measurement in the track mode

Commanded RPM (Track mode)	500 RPM			1000 RPM			2000 RPM		
Trial count	Trial 1	Trial 2	Trial 3	Trial 1	Trial 2	Trial 3	Trial 1	Trial 2	Trial 3
Measured Avg. RPM	500.14	495.77	503.09	990.78	986.34	999.41	1989.97	1994.85	2005.20
Speed (m/sec)	0.04329	0.04348	0.04337	0.08637	0.08621	0.08635	0.17306	0.17297	0.17297
Proportional Max. Speed (m/h)	2159.38	2187.88	2150.52	2159.38	2159.38	2155.45	2169.69	2163.26	2152.09

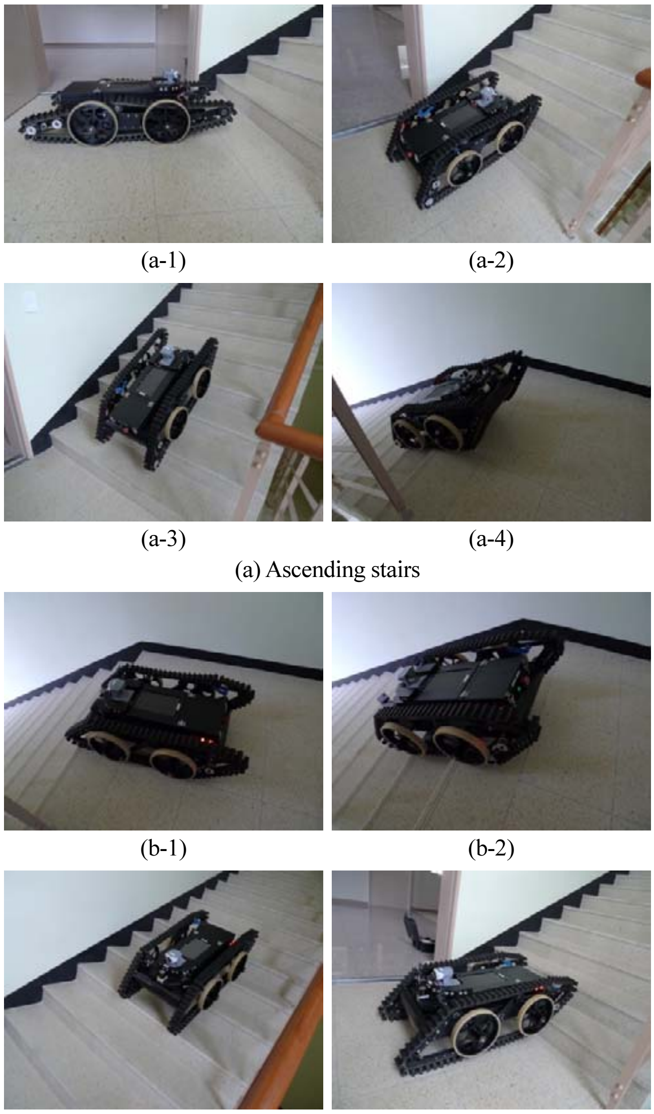

(a-1) (a-2) (a-3) (a-4)

(a) Ascending stairs

(b-1) (b-2) (b-3) (b-4)

(b) Descending stairs

Fig. 12 Consecutive process of ascending and descending stairs

Figure 12 shows the consecutive processes of ascending and descending the stairs by the wheel-track hybrid platform using the actual stairs of a building. The transformation is mainly achieved by the shape deformable track, which can be flattened or expanded to expose or hide the wheels. As a result, this hybrid platform can change the driving mode between a wheel mechanism and a track mechanism without an additional switchable or decouple mechanism. The wheel mechanism has good performance in turning flexibility and energy efficiency on the flat road. The transformable track mechanism has more prominent performance in off-road mobility. Combining their merits is the notion of this hybrid mechanism. In the beginning of this research, we focused on the simplicity in mechanical structure and the fast adaptability to irregular terrains. The experimental results showed that the simultaneous driving mechanism has advantage to improve the fast terrain-adaptive navigation performance in the urban environment where even roads and uneven off-road conditions coexist.

5. Conclusion

The proposed wheel-track hybrid robot aimed at not only rapid running over open ground but also the straightforward climbing of stairs. The former was achieved by wheel driving and the latter was accomplished by track transforming. The transformable track was mainly devised to maximize the driving torque so that the robot could easily overcome obstacles. The developed wheel-track hybrid robot platform is highly applicable to indoor environments containing floors, stairs, and other obstacles. With inexpensive PSD sensors, the autonomous attack angle estimation enabled the robot to transform the track intelligently according to the obstacle size. A combination of an inexpensive laser scanner, a readily available web camera, low-priced ultrasonic sensors, and a vibrating motor facilitated simple and intuitive control of the robot during tele-operation. Several experimental tests showed the strong potential that the terrain-adaptive wheel-track hybrid robot presented here is feasible for use in in actual applications.

Although tasks involving the overcoming of stairs and other obstacles are mainly discussed in this paper, our future work will focus on improving the autonomous navigation performance of the robot so that it can overcome various types of rough terrain and accomplish more advanced missions.

ACKNOWLEDGEMENT

This work was supported by the DGIST R&D Program of the Ministry of Education, Science and Technology of Korea (11-RS-01).

REFERENCES

1. Jeong, K., Kang, J., Lee, G., Lee, S., Seo, Y., Choi, C., Jung, S., and Kim, S., “Development of a robotic system for searching human victims in disasters,” Journal of Institute of Control, Robotics and Systems, Vol. 13, No. 1, pp. 41-45, 2007.
2. Chu, B., Jung, K., Han, C.-S., and Hong, D., “A survey of climbing robots: Locomotion and adhesion,” Int. J. Precis. Eng. Manuf., Vol. 11, No. 4, pp. 633-647, 2010.
3. Shen, S., Li, C., Cheng, C., Lu, J., Wang, S., and Lin, P., “Design of a leg-wheel hybrid mobile platform,” Proc. of the IEEE/RSJ International Conference on Intelligent Robots and Systems, pp. 4682-4687, 2009.
4. Choi, K. H., Jeong, H. K., Hyun, K. H., and Kwak, Y. K., “Obstacle negotiation for the rescue robot with variable single-tracked mechanism,” Journal of Institute of Control, Robotics and Systems, Vol. 13, No. 12, pp. 1222-1229, 2007.
5. Jacoff, A., Messina, E., and Evans, J., “A Standard Test Course for Urban Search and Rescue Robots,” Proc. of the Performance Metrics for Intelligent Systems Workshop, 2004.
6. Martens, J. D. and Newman, W. S., “Stabilization of a Mobile robot Climbing Stairs,” Proc. of the IEEE International Conference on Robotics and Automation, Vol. 3, pp. 2501-2507, 1994.
7. Kwon, H.-J., Shim, H., Kim, D.-G., Park, S.-K., and Lee, J. H., “A development of a transformable caterpillar equipped mobile robot,” International Conference on Control, Automation and Systems, pp. 1062-1065, 2007.
8. Lee, W. S., Kang, S. C., Kim, M. S., and Shin, K. C., “Rough terrain negotiable mobile platform with passively adaptive double-tracks and its application to rescue missions and EOD missions,” ICCAS, 2005.
9. iRobot®, “iRobot 510 PackBot,” http://www.irobot.com/en/us/robots/defense/packbot.aspx
10. Li, Z., Ma, S., Li, B., Wang, M., and Wang, Y., “Design and basic experiments of a transformable wheel-track robot with self-adaptive mobile mechanism,” Proc. of the IEEE/RSJ International Conference on Intelligent Robots and Systems, pp. 1334-1339, 2010.
11. Li, Z., Ma, S., Li, B., Wang, M., and Wang, Y., “Parameter Design and Optimization for Mobile Mechanism of a Transformable Wheel-Track Robot,” Proc. of the IEEE International Conference on Automation and Logistics, pp. 158-163, 2009.
12. Vysin, M. and Knoflicek, R., “The hybrid mobile robot,” Proc. of the IEEE International Conference on Industrial Technology, Vol. 1, pp. 262-264, 2003.
13. Elbit Systems, “Galileo military portable all terrain robot Viper by Elbit,” http://www.youtube.com/watch?v=o6rWfq6pX34
14. Lee, J.-W., Kim, B.-S., and Song, J.-B., “A Small Robot Based on Hybrid Wheel-Track Mechanism,” Transactions of the Korean Society of Mechanical Engineers A, Vol. 33, No. 6, pp.

545-551, 2009.

15. Michaud, F., Letourneau, D., Arsenault, M., Bergeron, Y., Cadrin, R., Gagnon, F., Legault, M. A., Millette, M., Pare, J. F., Tremblay, M. C., Lepage, P., Morin, Y., Bisson, J., and Caron, S., “Multi-Modal Locomotion Robotic Platform Using Leg-Track-Wheel Articulations,” Autonomous Robots, Vol. 18, No. 2, pp. 137-156, 2005.

16. BlueBotics, “Shrimp III,” http://www.bluebotics.com/solutions-/Shrimp/

17. Kim, Y.-G., Kim, J., Kwak, J.-H., Hong, D.-H., Lee, K.-D., and An, J., “Wheel &Track Hybrid Mobile Robot Platform and Mechanism for Optimal Navigation in Urban Terrain,” The Journal of Korea Robotics Society, Vol. 5, No. 3, pp. 270-277, 2010.

18. Kim, Y.-G., Kwak, J.-H., and An, J., “Terrain-adaptive and User-friendly Remote Control of Wheel-track Hybrid Mobile Robot Platform,” IEEE HRI’11, pp. 165-166, 2011.